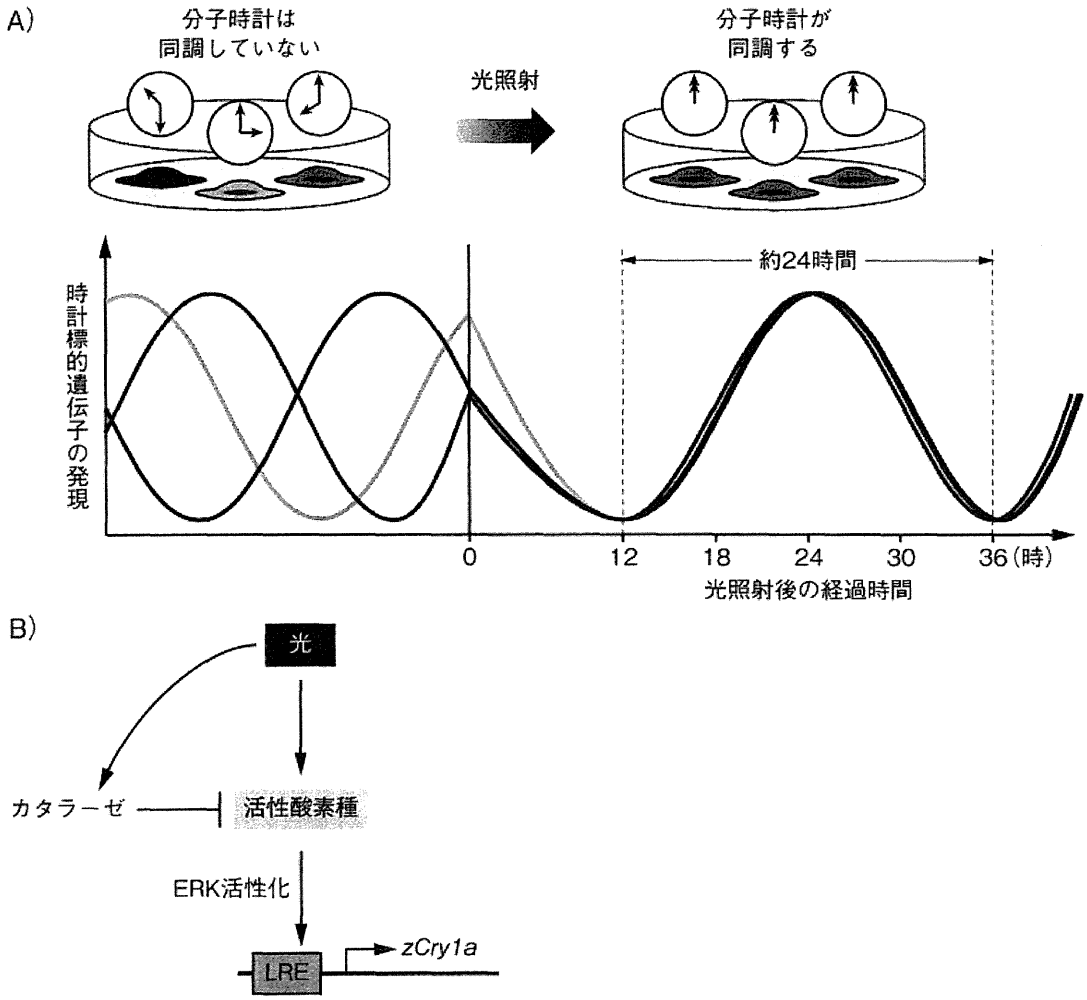

図3　ゼブラフィシュ分子時計の光同調機構
A）ゼブラフィシュ培養細胞に光照射処理を行うと，CLOCK：BMAL二量体の転写活性が光照射後約12時間まで抑制され，個々の分子時計が互いに同調する．B）光依存的な*zCry1a*の発現制御のモデル．LRE：light responsive element

す[2]．これらの知見は，分子時計による生理機能の日周的な調節が生体の恒常性維持に重要な役割を担っていることを示している．

2 活性酸素シグナルを介したゼブラフィシュ分子時計の光同調

哺乳動物の場合は，分子時計を同調させる光入力を感知できるのは目のみである．一方，ゼブラフィシュやショウジョウバエの末梢組織の細胞の分子時計は光に直接応答する[3) 11)]．分子時計は培養細胞にも存在し細胞自律的に制御されるが，通常の培養条件では各細胞の分子時計の周期の位相は互いに同調していない（**図3A**）．細胞に光照射を行うと，個々の分子時計の転写活性が最小値まで抑制され，各分子時計の周期の位相が互いに同調する[11)]．分子時計の光同調は光誘導され，CLOCK：BMAL二量体の転写を抑制するzCRY1aが担うが[3) 12)]，*zCry1a*の光依存的発現制御が活性酸素シグナルを介している可能性が報告されている[3)]．ゼブラフィシュ培養細胞に光照射を行うと活性酸素種が誘導される（**図3B**）．誘導された活性酸素種はERKシグナル経路の活性化を介して*zCry1a*遺伝子の転写を誘導する．一方で，*zCry1a*の誘導後，活性酸素種分解酵素カタラーゼ※1の発現量が光依存的に増加する．誘導されたカタラーゼは細胞内活性酸素種を

不活化し，*zCry1a*の発現量を負に調節することが示唆されている．

分子時計の光応答における活性酸素シグナルの関与は，ショウジョウバエにおいても報告されている[4]．ショウジョウバエのCRY（dCRY）は，光を直接受容しそのシグナルを分子時計に伝達する光受容体として機能するが，このシグナルの伝達には光依存的なdCRYの分解が主要な役割を担う．最近，このdCRYの光依存的な分解制御にかかわる因子のゲノムワイドのスクリーニングが行われ，グルタチオン*S*-トランスフェラーゼやチオレドキシンなどの細胞内酸化還元状態の制御因子がdCRYの光依存的分解の調節因子として同定されている．

3 活性酸素シグナルに依存したアカパンカビ分子時計の日周性形成

糸状菌アカパンカビの胞子形成には約24時間の周期性が観察されるが，この概日リズムはWHITE COLLAR-1（WC-1），WC-2，およびFREQUENCY（FRQ）より構成される分子時計〔FRQ/WC-1, WC-2 oscillator（FWO）〕により制御される（**図2**）[5)13)]．WC-1とWC-2の複合体〔WC-1-WC-2 complex（WCC）〕は*frq*遺伝子のプロモーターに結合しその発現を促進し，誘導されたFRQはWCCの転写活性を抑制する．

一方で，特定の条件で飼育したアカパンカビの*frq*変異体における遺伝子発現や胞子形成に概日リズムが観察されることが報告され，FRQに依存しない振動体〔FRQ-less oscillator（FLO）〕の存在が提唱されている[5)13)]．このFLOの生物学的役割に関しては現在まで明らかにされていない．アカパンカビにおいて，細胞内の活性酸素種のレベルはカラターゼの発現調節を介して概日的に制御されることが示唆されている[5)]．遺伝的な解析から，カラターゼの発現の周期性はWCCには依存するがFRQに依存しないことが示されている．一方で，WCCのDNA結合能，したがってその転写活性が，細胞内の活性酸素種のレベルに依存して制御される．以上より，「活性酸素種によるWCCの転写能の促進→WCCによるカタラーゼの誘導→カタラーゼによる活性酸素種レベルの抑制→WCCの転写活性の低下」というネガティブフィードバックループの存在が示唆され，このループはFLOの分子メカニズムの1つの候補と考えられる．

※1　カタラーゼ

抗酸化酵素の1つであり，2分子の過酸化水素を2分子の水と1分子の酸素に分解する反応を触媒する．この酵素は，ほぼすべての好気性生物に存在し，酸化ストレスから生物を守るうえで主要な役割を担っている．

4 哺乳動物細胞の酸化還元ホメオスタシスにおける時計タンパク質の役割

最近の研究により，*Bmal1*遺伝子のノックアウト（KO）細胞は野生型の細胞に比べて，酸化ストレスにより誘導される細胞老化や細胞増殖停止が促進することが報告されている[7)]．また，この酸化ストレスに対する感受性の亢進が，*Bmal1* KOマウスで観察される老化の促進および寿命の短縮という表現型の原因になる可能性が提唱されている[6)7)]．さらに，*Bmal1* KOマウスの脾臓，心臓，腎臓における活性酸素種レベルが増加することが明らかになっている[6)]．以上の知見より，BMAL1が分子時計または他の経路を介して細胞内酸化還元ホメオスタシスに関与すると考えられる．

哺乳動物においても活性酸素シグナルが分子時計の制御を担う可能性が提唱されている．例えば，哺乳動物のNPAS2（CLOCKのパラログ）とBMAL1の二量体のDNA結合能がNADの酸化還元状態に依存することが，生化学的な解析から明らかになっている[14)]．また，c-Jun N-terminal kinaseシグナル経路といった酸化ストレス応答性シグナル経路が，時計タンパク質の機能を制御することが報告されている[15)16)]．さらに，哺乳動物培養細胞を過酸化水素で処理すると分子時計の周期の位相が変化する[17)]ことから，哺乳動物の分子時計は活性酸素シグナルに応答できると考えられる．

5 細胞内酸化還元ホメオスタシス制御機構と分子時計の共進化の可能性

ペルオキシダーゼのPRXは細胞内で生成される過剰な活性酸素種を不活化し，生物を酸化ストレスから守る．PRXの活性はその酸化状態により調節されるが，最近の研究によりPRXの酸化還元状態が日周的に変動することが明らかにされ，この変動はPRXリズムとよばれる[8)9)]．PRXリズムは，細菌からヒトまでの多く

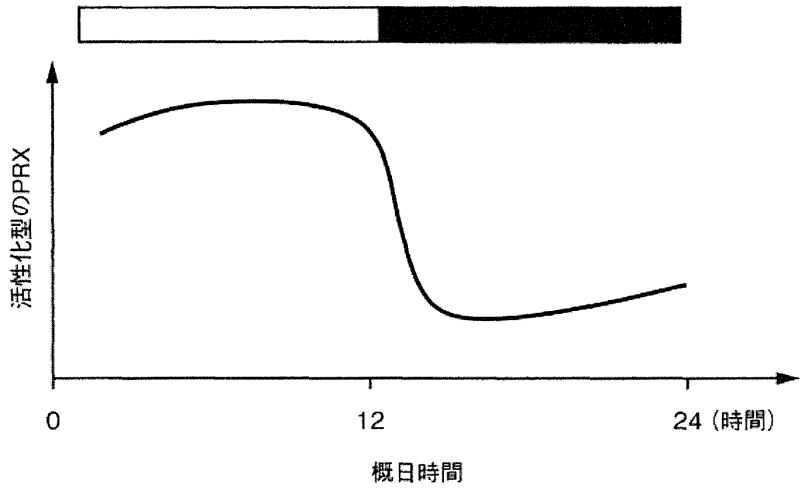

図4　PRX活性変動の日周性
PRXは酸化されると活性が負に制御される．グラフの縦軸は酸化されていないPRX（活性化型PRX）の量を表している．図中の白と黒のバーは，それぞれ主観的昼と主観的夜の時間帯を示している．概日時間とは，概日リズムの周期を24時間に見立て，24等分した時間制である．主観的昼のはじまりを概日時間の0時間，主観的夜のはじまりを12時間とする

の生物に共通に観察され，リズム周期の自律性，温度補償性，外環境周期への同調能という概日リズムの特性を有する．一方で，このリズムは，無核のヒト赤血球に存在することや阻害剤により転写を抑制しても継続することから，日周性の形成・維持に転写を必要としない．

興味深いことに，PRXリズムが細胞内酸化還元ホメオスタシス制御機構と分子時計の共進化により形成された可能性が提唱されている[9]．約25億年前の大酸化事変とよばれる時期に酸素が急速に蓄積し，好気性生物が地球上の主役となった．この時期の好気性生物にとって，PRXといった酸素呼吸の副産物として生じる活性酸素種を不活化するシステムの獲得は自然選択に有利に働いたと考えられる．また，分子時計をもつ最古の生物であるシアノバクテリアは大酸化事変と近い時期から地球上に存在しており，PRXと分子時計は進化の過程で近い時期に出現したと考えられる．

太陽光は酸素存在下で細胞内に活性酸素種を誘導するため，生物は外環境の明暗サイクルに依存して日周的に酸化ストレスにさらされてきた．初期の好気性生物は，PRXといった活性酸素種を取り除く機構と分子時計を共進化させることでPRXリズムを獲得し，太陽光による過酸化水素の誘導を予測してそれを効率的に不活化していたと考えられる．この考えを支持する知見として，系統樹解析からシアノバクテリアの分子時計制御因子（KaiA, KaiB, KaiC）とPRXが共進化したことが推測されている[9]．また，シアノバクテリアのPRXリズムにおいて，活性化型のPRXの量は生物が太陽光にさらされる主観的昼に高くなるように制御されている[9]（**図4**）．

おわりに

PRXリズムと分子時計は日周期形成の機構が互いに独立している．しかし，一方の機構を阻害すると他方の周期の位相や振幅が影響を受けることから，PRXリズムと分子時計がクロストークすることが報告されている[8)9)]．このクロストークの分子メカニズムや生物学的意義の解明は，活性酸素シグナルと概日リズムの関連ならび概日リズムの進化的起源に関する理解に貢献すると考えられる．

文献

1）Okamura, H. : J. Biol. Rhythms, 19 : 388-399, 2004
2）Sahar, S. & Sassone-Corsi, P. : Nat. Rev. Cancer, 9 : 886-896, 2009
3）Hirayama, J. et al. : Proc. Natl. Acad. Sci. USA, 104 : 15747-15752, 2007
4）Sathyanarayanan, S. et al. : Genes Dev., 22 : 1522-1533, 2008
5）Yoshida Y. et al. : PLoS ONE, 22 : 1522-1533, 2011

6) Kondratov, R. V. et al. : Genes Dev., 20 : 1868-1873, 2006
7) Khapre, R. V. et al. : Cell Cycle, 10 : 4162-4169, 2011
8) O'Neill, J. S. & Reddy, A. B. : Nature, 469 : 498-503, 2011
9) Edgar, R. S. et al. : Nature, 485 : 459-464, 2012
10) Nakajima, M. et al. : Science, 308 : 414-415, 2005
11) Carr, A. J. & Whitmore, D. : Nat. Cell Biol., 7 : 319-321, 2005
12) Tamai, T. K. et al. : Proc. Natl. Acad. Sci. USA, 104 : 14712-14717, 2007
13) Dunlap, J. C. & Loros, J. J. : Curr. Opin. Microbiol., 9 : 579-587, 2006
14) Rutter, J. et al. : Science, 293 : 510-514, 2001
15) Yoshitane, H. et al. : EMBO Rep., 13 : 455-461, 2012
16) Uchida, Y. et al. : J. Biol. Chem., 287 : 8318-8326, 2012
17) Oklejewicz, M. et al. : Curr. Biol., 18 : 286-291, 2008

＜筆頭著者プロフィール＞
平山　順：2003年 京都大学大学院人間・環境学研究科修了（池永満生教授および藤堂 剛教授）．2003年～2006年 仏国 Institut de Génétique et de Biologie Moléculaire et Cellulaire，2006年～2008年 米国 University of California Irvine にて博士研究員（Dr. Sasssone-Corsi Paolo）．2008年～2010年 東京医科歯科大学難治疾患研究所 MTT プログラム特任講師を経て，東京医科歯科大学難治疾患研究所発生再生生物学分野，准教授．

モデル生物を用いた肝発生および肝サイズ制御機構の解明

宮村憲央* 仁科博史*

索引用語：肝発生，モデル生物，小型魚類，器官サイズ，肝癌

1 はじめに

肝発生に関与する遺伝子やシグナル分子は多数のノックアウトマウスの作出によって次々と明らかにされている．また小型魚類を用いた解析からも新たな知見が得られつつある．

本稿ではマウスや小型魚類を用いて明らかとなった肝発生機構について概説する．また最近明らかとなった器官サイズ制御シグナルによる肝サイズおよび肝癌抑制の制御機構についても紹介する．

2 マウスを用いた肝発生研究

マウス個体は受精後約20日で出生し，成体へと成長する(図1A)．胎齢8日目に心臓中胚葉からのFGFシグナル，横中隔間充織からのBMPシグナルによって，前腸内胚葉の一部が肝臓の予定領域となる(肝特異化，図1B)[1]．胎齢9日目に特異化された領域に肝芽細胞が出現し，胎齢10日目には横中隔領域に細胞が増殖，浸潤し肝芽を形成する．この頃に造血幹細胞が肝臓へ流入し，胎仔期の肝臓は主要な造血組織として機能する．

肝芽細胞は自己増殖能と細胞分化能(肝細胞および胆管上皮細胞に分化する能力)を有し，幹細胞としての役割を担う(図2)．この肝芽細胞の分化や増殖を制御する分子は各種ノックアウトマウスの解析から明らかにされてきた[1]．Foxa1とFoxa2の前腸内胚葉特異的ダブルノックアウトマウスでは肝芽細胞への分化が障害され肝芽が形成されない[2]．Tbx3のノックアウトマウスは肝芽細胞の増殖異常により肝臓の低形成を示す[3]．Prox1のノックアウトマウスは肝芽細胞の横中隔領域への浸潤が起こらず，肝臓形成不全となる[4]．そのほか，ストレス応答性キナーゼMKK4やMKK7のノックアウトマウスは肝芽細胞の増殖異常を示す[5]．

肝芽細胞から肝細胞および胆管上皮細胞への分化，成熟を制御する分子はノックアウトマウスや*in vitro*培養系を用いて明らかとされている[1,6]．転写因子C/EBP αのノックアウトマウスは肝細胞での代謝酵素の発現が不

Norio MIYAMURA et al: Regulation of liver development and size: lessons from animal models
*東京医科歯科大学難治疾患研究所 発生再生生物学分野［〒113-8510 東京都文京区湯島1-5-45］

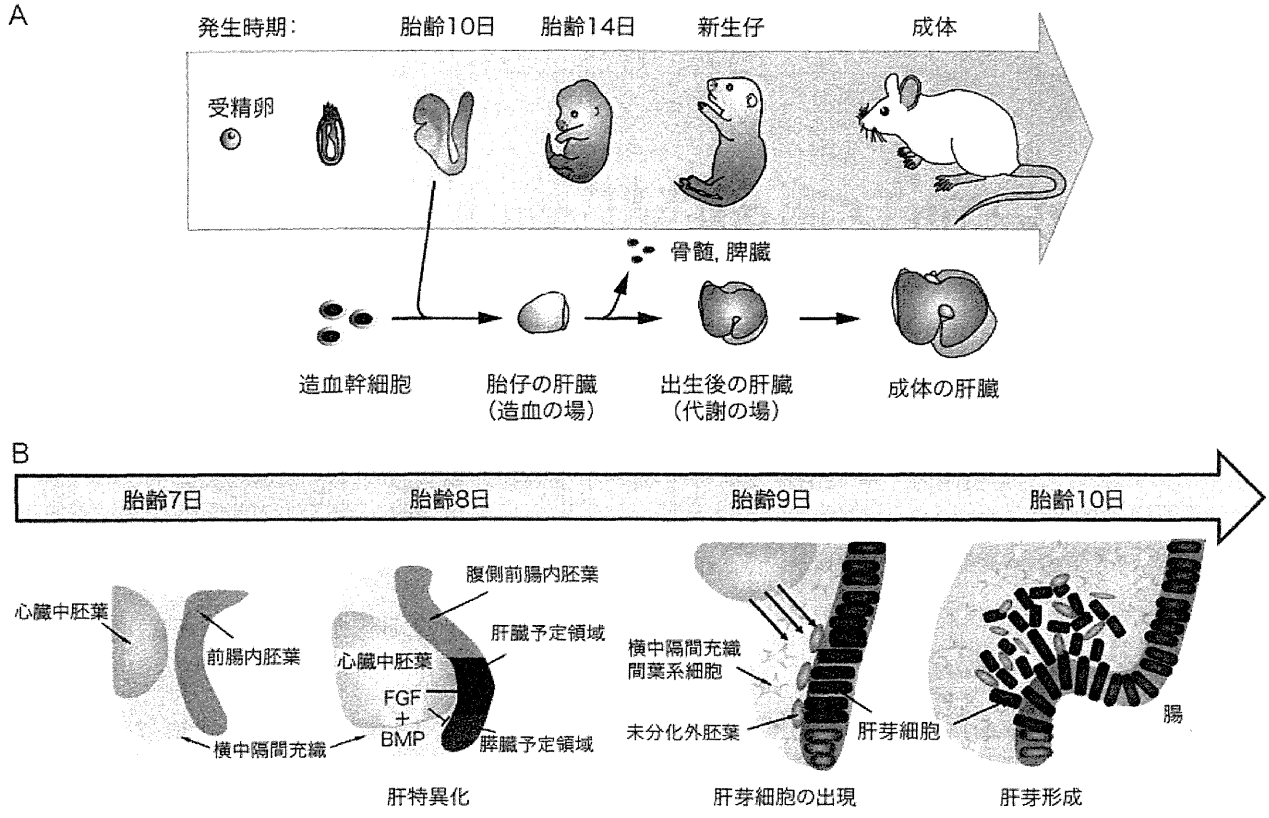

図1　マウスの発生と肝発生

A：マウスは約20日で出生し成体へと成長する．胎仔期の肝臓には造血細胞が流入し造血の場として機能する．出生後の肝臓は代謝の場として機能する．

B：胎齢8日目に心臓中胚葉からのFGFシグナル，横中隔間充織からのBMPシグナルが前腸内胚葉に伝達されることで肝臓の予定領域が決定される(肝特異化)．胎齢9日目には肝芽細胞が出現し，胎齢10日目に肝芽が形成される．

全となり，出生直後に低血糖と高アンモニア血症を示して死亡する[7]．Hnf4を欠損する肝芽細胞の初代培養細胞は肝細胞への分化が障害される[8]．また，肝芽細胞の初代培養系にOSMを添加することで肝細胞分化が強く誘導されることが示されている．Hnf6, Hnf1 β のそれぞれのノックアウトマウスは胆管形成異常を示し，Jagged-Notchシグナル伝達系は，Hnf6, Hnf1 β の上流分子として発現を制御する可能性が示唆されている[9]．

血液・免疫研究では300以上の細胞表面抗原が単離され，細胞の同定，分取が高分解能で行われているのとは対照的に，肝臓研究では，細胞表面マーカーの単離が進んでおらず，細胞の分取，同定の解析が遅れている．胎仔肝に発現する分子として分泌性の糖蛋白質AFPがよく知られているが，セルソーティングで細胞を単離するには不向きである．そのため細胞表面マーカーの単離が精力的になされている．肝芽細胞に特異的に発現する分子として，EGFリピートを持つ細胞膜蛋白質Dlk1が単離されている[10]．また上皮細胞接着分子EpCAMは，内胚葉細胞と肝芽細胞に発現する[11]．EpCAMは徐々に発現が低下していくが，胆管上皮細胞に分化すると再び発現誘導されるユニークな分子である．ヒトの肝芽細胞でもDlk1，EpCAMは細胞表面マーカーとして利用できる．そのほか，マウ

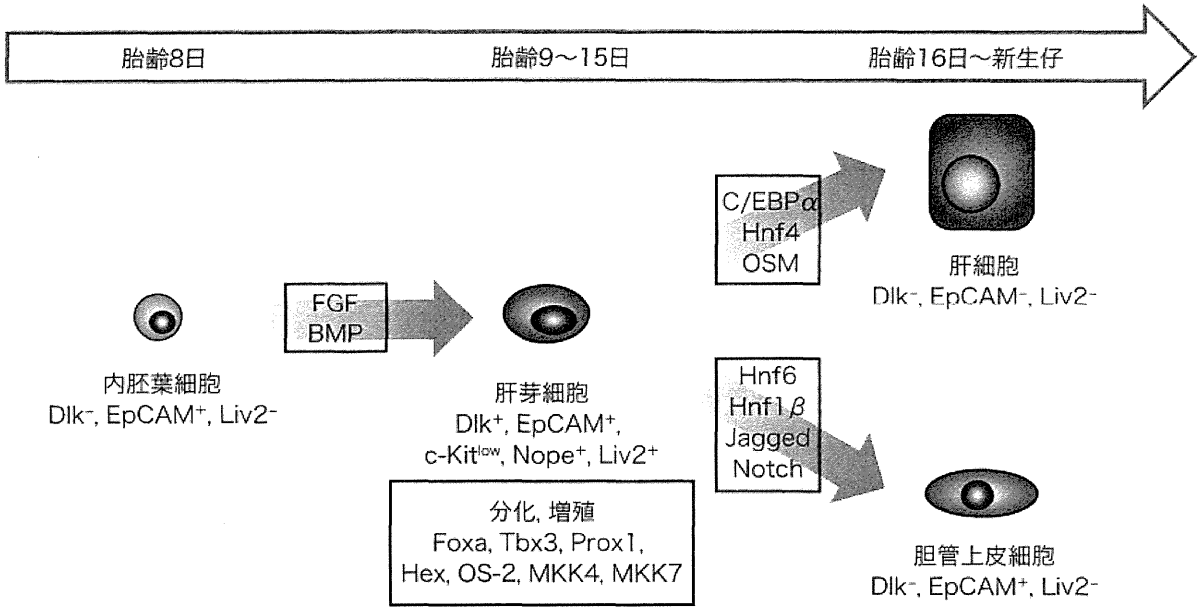

図2　肝構成細胞の発生と関連分子の発現

内胚葉細胞から分化した肝芽細胞は肝細胞と胆管上皮細胞への分化能を有している．肝芽細胞の分化，増殖を担うシグナルはFoxa, Tbx3, Prox1, Hex, OS-2, MKK4, MKK7が関与する．肝細胞への分化はC/EBP α, Hnf4, OSMが，胆管への分化はHnf6, Hnf1 β, Jagged, Notchが関与する．内胚葉細胞はEpCAMを発現し，肝芽細胞はDlk1，Nope，Liv2を特異的に発現する．肝細胞はEpCAMを発現しないが，胆管上皮細胞はEpCAMを発現する．

スの肝芽細胞はc-Kitを弱く発現していることやイムノグロブリンスーパーファミリーのNopeを発現していることが明らかとなっている[12]．また肝芽細胞特異的な抗体としてLiv2抗体が報告されている[13]．このように各分化過程の表面抗原マーカーが単離され，現在では各分化段階の細胞を同定しセルソーターで単離することが可能になり，*in vitro*の分化誘導実験に大変貢献している．

3　小型魚類を用いた肝発生研究

脊椎動物のゼブラフィッシュやメダカなどの小型魚類は，肝臓や胆嚢，膵臓，心臓や腎臓など哺乳動物と同様の器官を有している（図3）．また卵生で胚が透明なため，肝形成過程を生きたまま経時的に観察できること，ゲノムサイズが小さいこと，飼育スペースが節約できること，突然変異体の大規模スクリーニングが可能であることなど研究上の利点をもつ．

1．ゼブラフィッシュを用いた肝研究

1990年代初頭に，ドイツのチュービンゲンとアメリカのボストンで大規模な変異体スクリーニングが行われ，数百に及ぶ変異体が単離された．消化器系に異常を示すゼブラフィッシュ変異体も単離されており，そのうち肝形成に関与するものとして10種類以上が単離された[14,15]．またStainierらのグループは内胚葉でGFPが発現するトランスジェニック系統を樹立し，GFPの蛍光を利用して，肝臓の出芽形成や形態を詳細に解析可能な実験系を確立した[16]．これを用いて肝臓の特異化に異常を示す*prometheus*変異体が単離された．原因遺伝子の同定より*prometheus*変異体は*Wnt2bb*を欠損することがわかり，FgfおよびBmpシグナルの上流にWntシグナ

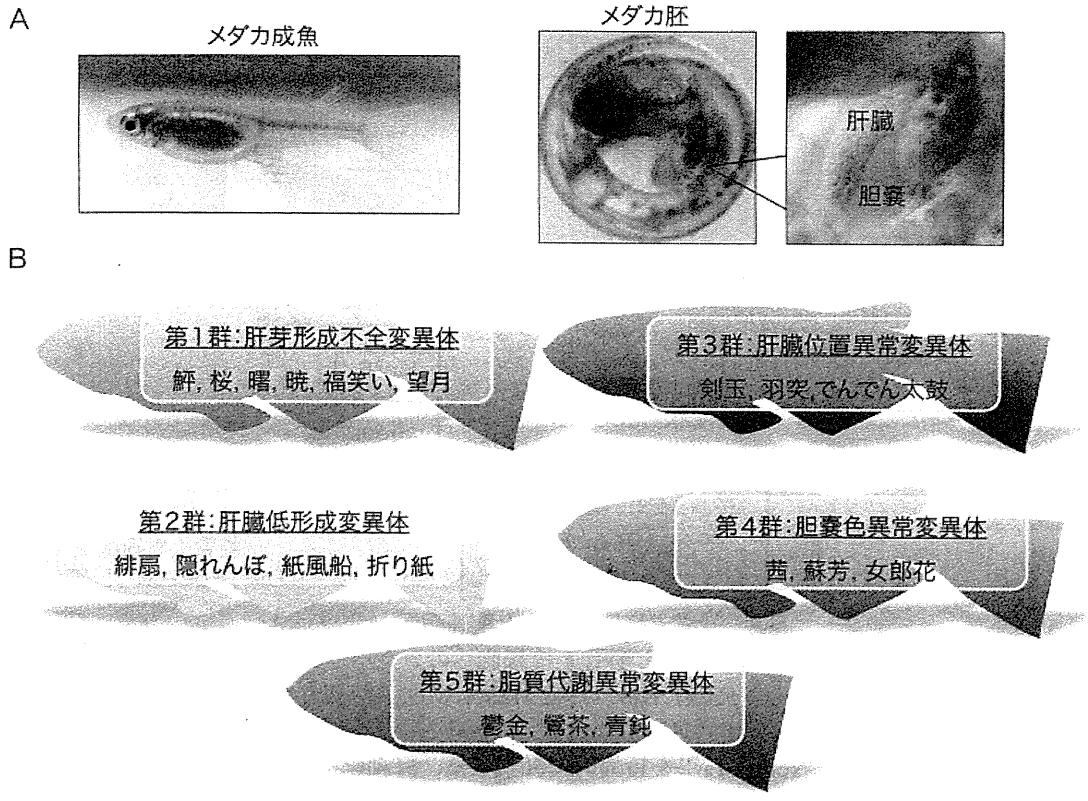

図3　肝形成および肝機能不全メダカ変異体
A：メダカ成魚とメダカ胚を示す．初期胚は肝臓，胆嚢を実体顕微鏡で観察できる．
B：メダカ大規模スクリーニングにより単離された肝形成・肝機能不全変異体の分類と変異体名．すべて和名で名付けられている．

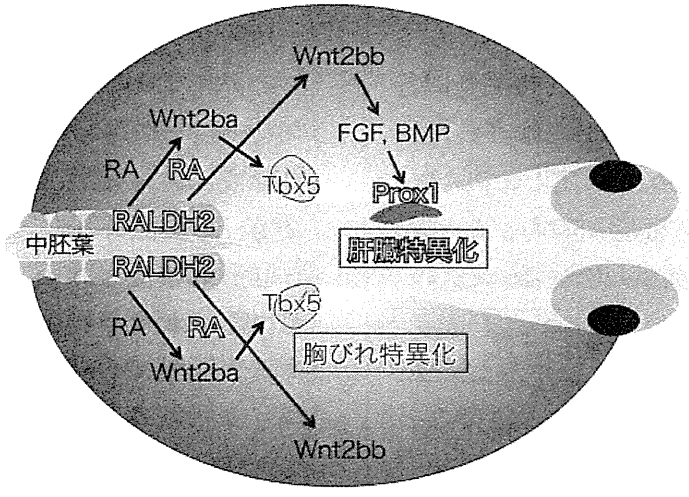

図4　メダカの肝特異化と胸鰭特異化制御機構
レチノイン酸(RA)とWntシグナル伝達系がTbx5の発現を介して胸鰭の特異化を決定する．一方，RAとWntシグナル伝達系がFGF，BMPを介してProx1の発現を誘導し肝臓の特異化を行う．

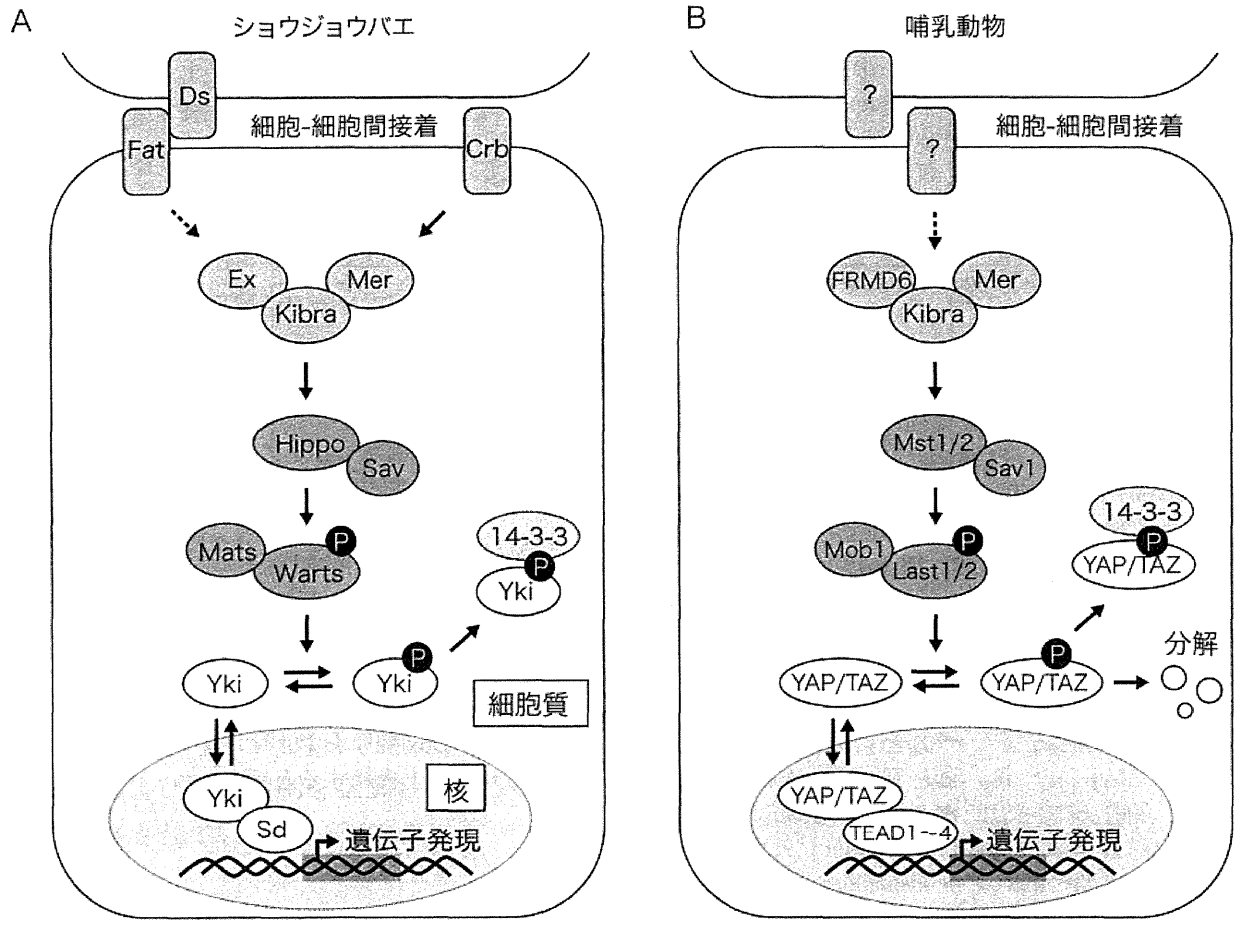

図5　ショウジョウバエと哺乳動物のHippoシグナル伝達系

A：ショウジョウバエのHippoシグナル伝達系はYkiをリン酸化しYkiを細胞質へ留める．脱リン酸化型のYkiは核内へ移行し，転写因子Sdと結合し遺伝子発現を誘導する．

B：Hippoシグナル伝達系はマウスやヒトなどの哺乳動物でも高度に保存されている．

ル伝達系が存在していることが明らかになった(図4)．

2. メダカを用いた肝研究

1990年代の終わりに国産のモデル生物メダカを用いた大規模スクリーニングが始まった[17]．われわれのグループもこのプロジェクトに参画し，肝形成や肝機能不全変異体を複数単離することに成功した(図3B)[18]．得られた19種の変異体は，その表現型から5つのグループ(第1群：肝芽形成不全，第2群：肝臓低形成，第3群：肝臓位置異常，第4群：胆嚢色異常，第5群：脂質代謝異常)に分類された．このうち第2群に属する緋扇(*hiohgi*)変異体は肝臓の低形成および胸鰭の消失という興味深い表現型を示す．原因遺伝子の同定により，ビタミンAからオールトランスレチノイン酸(RA)を合成する酵素(レチノイン酸合成酵素タイプ2，RALDH2)をコードする遺伝子の変異であることが判明した[19]．*hiohgi*変異体を用いた解析からRALDH2がRAを産生し，*Wnt2bb*遺伝子の発現を側板中胚葉に誘導することにより，肝臓の特異化が決定されることが示された(図4)．RALDH2のノックアウトマウスおよびゼブラフィッシュは肝形成以前に致死となることから，肝形成におけるRALDH2の役割については未解明で

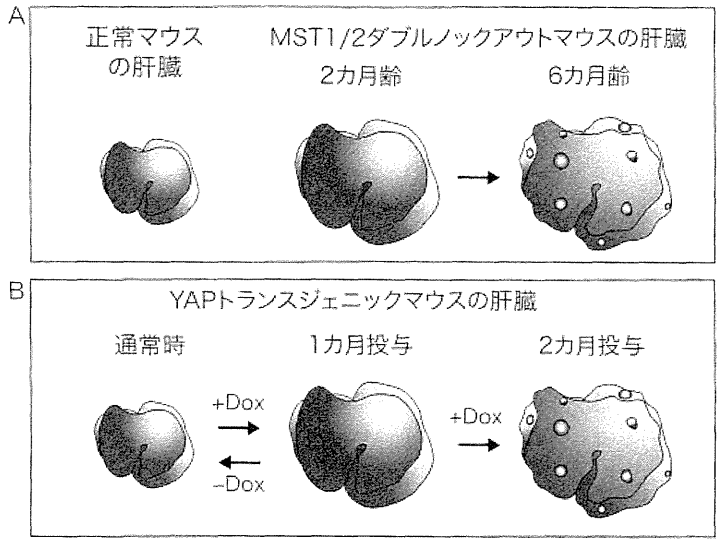

図6　Hippoシグナル伝達系の破綻による肝サイズ増大と肝癌発症
A：2カ月齢のMst1とMst2のダブルノックアウトマウスの肝臓は正常の肝臓と比較して5倍まで増大し，6カ月後には肝癌を発症する．
B：YAPトランスジェニックマウスにDox投与でYAPの発現を誘導すると1カ月で肝重量が5倍まで増大する．Dox投与を中止すると元の大きさに戻るが，Dox投与を2カ月以上継続すると肝癌を発症する．

あった．メダカを用いた研究からRALDH2が肝特異化の制御に関与することが明らかにされた．

4　肝サイズおよび肝癌抑制の制御

2003年にショウジョウバエを用いた研究から器官サイズを制御するHippoシグナル伝達系が明らかになった(図5A)[20]．Hippoシグナル伝達系はセリンスレオニンキナーゼHippoを中心とするリン酸カスケードでありHippoが活性化されると最終標的分子の転写共役因子Ykiがリン酸化される．リン酸化されたYkiは細胞質で14-3-3と結合することで細胞質に局在化する．一方，リン酸化されていないYkiは，核内で転写因子と共役し遺伝子発現を亢進させる．器官のサイズを変化させるには，構成する細胞の数を制御するか，細胞の大きさを制御する2つの可能性が考えられる．Hippoシグナル伝達系は，細胞増殖や細胞死に関する遺伝子の発現を制御することで，細胞の数を制御している．このHippoシグナル伝達系は哺乳類にも高度に保存されており，HippoはMst1やMst2（Mst1/2），YkiはYAPやTAZと相同遺伝子の関係にある(図5B)．

興味深いことに，Hippoシグナル伝達系の構成遺伝子の多くはヒトの癌抑制遺伝子として単離された経緯があり，癌抑制シグナル伝達系とも呼ばれている．また細胞機能としては細胞接触障害(Contact inhibition)や上皮間葉転換(Epithelial-Mesenchymal Transition: EMT)，幹細胞維持に関与することが報告されている．

Hippoシグナル伝達系の肝臓での機能がノックアウトマウスやトランスジェニックマウスの作出によって明らかにされている．

Mst1とMst2の肝臓特異的ダブルノックアウトマウスは，生後2カ月で正常な肝臓よりサイズが5倍まで増大し，生後3～6カ月で肝癌を発症する(図6A)[21~23]．また，ドキシサイクリン(Dox)依存的に肝臓でYAPを過剰発現するトランスジェニックマウスは，Doxを投与することで，肝臓のサイズが約5倍まで増大する[24,25]．興味深いことに，Dox投与を中止すると元のサイズまで戻るが，2カ月以上の長期間にわたってDoxを投与すると肝癌を発症する(図6B)．さらにSav1や*Nf2*遺伝子がコードするMerなど他のHippoシグナル伝達系構成遺伝子のノックアウトマウスでも肝臓サイズの増大と肝癌の発症が報告されている．このように，Hippoシグナル伝達系は肝臓においてYAPを負に制御することで肝サイズおよび肝癌抑制を制御していることが強く示唆されている[26]．

5 おわりに

肝発生に関する基礎研究の成果は肝再生研究にも応用されている．最近，線維芽細胞にFoxaとHnf6を発現させることで肝細胞様の細胞(iHep細胞：induced hepatocyte-like cells)を作出できることが報告された[27]．

ノックアウトマウスの作出や細胞表面マーカーを利用した細胞分離技術の向上が，昨今の肝発生研究の進展を強力に後押ししている．また小型魚類での研究成果は，胎生である哺乳動物の短所を補っている．さらに，肝臓を持たないショウジョウバエから得られた知見が肝サイズや肝癌の抑制機構の解明に繋がったことは興味深い．さまざまなモデル生物を上手く利用することの重要性を示している．

文　献

1) Zaret KS, Grompe M : Generation and regeneration of cells of the liver and pancreas. Science 322 : 1490–1494, 2008
2) Lee CS, Friedman JR, Fulmer JT et al : The initiation of liver development is dependent on Foxa transcription factors. Nature 435 : 944–947, 2005
3) Suzuki A, Sekiya S, Büscher D et al : Tbx3 controls the fate of hepatic progenitor cells in liver development by suppressing p19ARF expression. Development 135 : 1589–1595, 2008
4) Sosa-Pineda B, Wigle JT, Oliver G : Hepatocyte migration during liver development requires Prox1. Nat Genet 25 : 254–255, 2000
5) Nakamura T, Nishina H : Liver development: lessons from knockout mice and mutant fish. Hepatol Res 39 : 633–644, 2009
6) Kamiya A, Kinoshita T, Ito Y et al : Fetal liver development requires a paracrine action of oncostatin M through the gp130 signal transducer. EMBO J 18 : 2127–2136, 1999
7) Wang N, Finegold M, Bradley A et al : Impaired energy homeostasis in C/EBP alpha knockout mice. Science 269 : 1108–1112, 1995
8) Hayhurst GP, Strick-Marchand H, Mulet C et al : Morphogenetic competence of HNF4 alpha-deficient mouse hepatic cells. J Hepatol 49 : 384–395, 2008
9) Tanaka M, Itoh T, Tanimizu N et al : Liver stem/progenitor cells: their characteristics and regulatory mechanisms. J Biochem 149 : 231–239, 2011
10) Tanimizu N, Nishikawa M, Saito H et al : Isolation of hepatoblasts based on the expression of Dlk/Pref-1. J Cell Sci 116 : 1775–1786, 2003
11) Tanaka M, Okabe M, Suzuki K et al : Mouse hepatoblasts at distinct developmental stages are characterized by expression of EpCAM and DLK1: drastic change of EpCAM expression during liver development. Mech Dev 126 : 665–676, 2009
12) Nierhoff D, Levoci L, Schulte S et al : New cell surface markers for murine fetal hepatic stem cells identified through high density complementary DNA microarrays. Hepatology 46 : 535–547, 2007
13) Watanabe T, Nakagawa K, Ohata S et al :

SEK1/MKK4-mediated SAPK/JNK signaling participates in embryonic hepatoblast proliferation via a pathway different from NF-kappaB-induced anti-apoptosis. Dev Biol 250 : 332–347, 2002
14) Chen JN, Haffter P, Odenthal J et al : Mutations affecting the cardiovascular system and other internal organs in zebrafish. Development 123 : 293–302, 1996
15) Pack M, Solnica-Krezel L, Malicki J et al : Mutations affecting development of zebrafish digestive organs. Development 123 : 321–328, 1996
16) Field HA, Ober EA, Roeser T et al : Formation of the digestive system in zebrafish. I. Liver morphogenesis. Dev Biol 253 : 279–290, 2003
17) Furutani-Seiki M, Sasado T, Morinaga C et al : A systematic genome-wide screen for mutations affecting organogenesis in Medaka, Oryzias latipes. Mech Dev 121 : 647–658, 2004
18) Watanabe T, Asaka S, Kitagawa D et al : Mutations affecting liver development and function in Medaka, Oryzias latipes, screened by multiple criteria. Mech Dev 121 : 791–802, 2004
19) Negishi T, Nagai Y, Asaoka Y et al : Retinoic acid signaling positively regulates liver specification by inducing wnt2bb gene expression in medaka. Hepatology 51 : 1037–1045, 2010
20) Pan D : The hippo signaling pathway in development and cancer. Dev Cell 19 : 491–505, 2010
21) Lu L, Li Y, Kim SM et al : Hippo signaling is a potent in vivo growth and tumor suppressor pathway in the mammalian liver. Proc Natl Acad Sci USA 107 : 1437–1442, 2010
22) Zhou D, Conrad C, Xia F et al : Mst1 and Mst2 maintain hepatocyte quiescence and suppress hepatocellular carcinoma development through inactivation of the Yap1 oncogene. Cancer Cell 16 : 425–438, 2009
23) Song H, Mak KK, Topol L et al : Mammalian Mst1 and Mst2 kinases play essential roles in organ size control and tumor suppression. Proc Natl Acad Sci USA 107 : 1431–1436, 2010
24) Dong J, Feldmann G, Huang J et al : Elucidation of a universal size-control mechanism in Drosophila and mammals. Cell 130 : 1120–1133, 2007
25) Camargo FD, Gokhale S, Johnnidis JB et al : YAP1 increases organ size and expands undifferentiated progenitor cells. Curr Biol 17 : 2054–2060, 2007
26) Avruch J, Zhou D, Fitamant J et al : Mst1/2 signalling to Yap: gatekeeper for liver size and tumour development. Br J Cancer 104 : 24–32, 2011
27) Sekiya S, Suzuki A : Direct conversion of mouse fibroblasts to hepatocyte-like cells by defined factors. Nature 475 : 390–393, 2011

*　　*　　*

Highly Purified Eicosapentaenoic Acid Increases Interleukin-10 Levels of Peripheral Blood Monocytes in Obese Patients With Dyslipidemia

NORIKO SATOH-ASAHARA, MD, PHD[1]
AKIRA SHIMATSU, MD, PHD[1,2]
YOUSUKE SASAKI, BSC[1]
HIDENORI NAKAOKA, PHD[1]
AKIHIRO HIMENO, MD[1]
MAYU TOCHIYA, MD[3]
SHIGEO KONO, MD, PHD[1,3]
TOMOHIDE TAKAYA, PHD[2]
KOH ONO, MD, PHD[4]
HIROMICHI WADA, MD, PHD[2]
TAKAYOSHI SUGANAMI, MD, PHD[5]
KOJI HASEGAWA, MD, PHD[2]
YOSHIHIRO OGAWA, MD, PHD[5,6]

OBJECTIVE—It has recently been highlighted that proinflammatory (M1) macrophages predominate over anti-inflammatory (M2) macrophages in obesity, thereby contributing to obesity-induced adipose inflammation and insulin resistance. A recent clinical trial revealed that highly purified eicosapentaenoic acid (EPA) reduces the incidence of major coronary events. In this study, we examined the effect of EPA on M1/M2-like phenotypes of peripheral blood monocytes in obese dyslipidemic patients.

RESEARCH DESIGN AND METHODS—Peripheral blood monocytes were prepared from 26 obese patients without and 90 obese patients with dyslipidemia. Of the latter 90 obese patients with dyslipidemia, 82 patients were treated with or without EPA treatment (1.8 g daily) for 3 months.

RESULTS—Monocytes in obese patients with dyslipidemia showed a significantly lower expression of interleukin-10 (IL-10), an M2 marker, than those without dyslipidemia. EPA significantly increased serum IL-10 and EPA levels, the EPA/arachidonic acid (AA) ratio, and monocyte IL-10 expression and decreased the pulse wave velocity (PWV), an index of arterial stiffness, compared with the control group. After EPA treatment, the serum EPA/AA ratio was significantly correlated with monocyte IL-10 expression. Only increases in monocyte IL-10 expression and serum adiponectin were independent determinants of a decreased PWV by EPA. Furthermore, EPA significantly increased the expression and secretion of IL-10 in human monocytic THP-1 cells through a peroxisome proliferator–activated receptor (PPAR)γ-dependent pathway.

CONCLUSIONS—This study is the first to show that EPA increases the monocyte IL-10 expression in parallel with decrease of arterial stiffness, which may contribute to the antiatherogenic effect of EPA in obese dyslipidemic patients.

Diabetes Care 35:2631–2639, 2012

The monocyte–macrophage system plays a role in the pathogenesis of obesity and atherosclerotic disease (1,2). This system shows at least two distinct phenotypes of differentiation: proinflammatory (M1) and anti-inflammatory (M2) (3). It has been reported that, in obese adipose tissue, macrophage accumulation is increased, and proinflammatory M1 macrophages predominate over anti-inflammatory M2 macrophages, thereby contributing to obesity-induced adipose inflammation and insulin resistance (4–6). The expression of both M1 and M2 markers is detected in peripheral blood mononuclear cells and even in atherosclerotic plaques (7,8). We and others also provided evidence for the inflammatory state and unfavorable M1/M2-like phenotypes of peripheral blood monocytes in obese diabetic patients (9,10). In particular, interleukin-10 (IL-10), an anti-inflammatory cytokine and M2 marker, might be involved in M2 macrophage recruitment, thus contributing to reducing inflammation and improving the insulin signal (5,11).

In epidemiological and clinical trials, fish oil and omega-3 (n-3) polyunsaturated fatty acids (PUFAs) were found to reduce the incidence of coronary heart disease (12). A large-scale, prospective, randomized clinical trial, the Japan Eicosapentaenoic Acid Lipid Intervention Study (JELIS), demonstrated that highly purified eicosapentaenoic acid (EPA), a specific n-3 PUFA used clinically to treat dyslipidemia, significantly reduces the incidence of major coronary events via cholesterol-independent mechanisms (13). As antiatherogenic effects, we previously demonstrated that EPA reduces atherogenic lipoproteins and C-reactive protein (CRP), an inflammatory marker, as well as the pulse wave velocity (PWV), an index of arterial stiffness, and increases the secretion of adiponectin, the only established adipocytokine with anti-inflammatory and antiatherogenic properties, in obese patients (14–16). We also reported that EPA markedly inhibits LPS-induced monocyte adhesion to the aortic endothelium in parallel with the suppression of endothelial adhesion molecules intracellular adhesion molecule-1 and vascular cell adhesion molecule-1 (17). Several studies showed that dietary n-3 PUFAs and EPA inhibit the ability of macrophages to secrete several effector

From the [1]Division of Diabetic Research, National Hospital Organization, Kyoto Medical Center, Kyoto, Japan; [2]Translational Research, Clinical Research Institute, National Hospital Organization, Kyoto Medical Center, Kyoto, Japan; the [3]Diabetes Center, National Hospital Organization, Kyoto Medical Center, Kyoto, Japan; the [4]Department of Cardiovascular Medicine, Graduate School of Medicine, Kyoto University, Kyoto, Japan; the [5]Department of Molecular Medicine and Metabolism, Medical Research Institute, Graduate School of Medical and Dental Sciences, Tokyo Medical and Dental University, Tokyo, Japan; and the [6]Department of Molecular Endocrinology and Metabolism, Graduate School of Medical and Dental Sciences, Tokyo Medical and Dental University, Tokyo, Japan.
Corresponding author: Noriko Satoh-Asahara, norikos@oregano.ocn.ne.jp.
Received 8 February 2012 and accepted 14 June 2012.
DOI: 10.2337/dc12-0269. Clinical trial reg. no. UMIN 000000559, www.umin.ac.jp/ctr/.
This article contains Supplementary Data online at http://care.diabetesjournals.org/lookup/suppl/doi:10.2337/dc12-0269/-/DC1.

molecules that may be involved in the pathogenesis of atherosclerosis (18,19). Given these protective effects of n-3 PUFAs and EPA on the monocyte–macrophage system (17–19), it is tempting to speculate on the beneficial effect of EPA on the M1/M2-like phenotypes of peripheral blood monocytes in obese patients during the progression of atherosclerosis; however, no direct evidence for such an effect of EPA has been established. EPA can be metabolized to anti-inflammatory eicosanoids and also competitively inhibits the production of arachidonic acid (AA), an n-6 PUFA, and inflammatory eicosanoids derived from AA, which is the precursor of important molecules involved in inflammation and atherosclerotic process (20). Subanalysis of JELIS and other studies suggested that a decreased serum EPA/AA ratio is significantly associated with the incidence of cardiac death and myocardial infarction and the coronary plaque score (21,22).

In this study, we demonstrate for the first time that EPA increased IL-10 RNA expression in peripheral blood monocytes of obese patients with dyslipidemia in parallel with the decrease of arterial stiffness. In addition, the serum EPA/AA ratio after EPA treatment was significantly correlated with IL-10 RNA expression of monocytes. Furthermore, EPA enhanced the expression level of IL-10 RNA through peroxisome proliferator–activated receptor (PPAR)γ in vitro. As EPA reduced the risk of major coronary events in a large-scale, prospective, randomized clinical trial (13), this study provides important insight into its therapeutic implications for obesity-related metabolic sequelae and cardiovascular disease.

RESEARCH DESIGN AND METHODS

Subjects

A total of 116 Japanese obese outpatients were recruited in our clinic during the period from January 2008 to January 2009. Obese patients were defined as those with a BMI of ≥25 kg/m^2, based on the guideline proposed by the Japan Society for the Study of Obesity. Patients with severe renal diseases and severe liver dysfunction were excluded from this study. Patients taking statins, fibrates, angiotensin-converting enzyme inhibitors, angiotensin II receptor antagonists, insulin-sensitizing agents, or insulin therapy were excluded from the study. All other medications were continued and remained unchanged during the study protocol. This study is a part of the Japan Obesity and Metabolic Syndrome Study, which has undergone clinical trial registration in the University Hospital Medical Information Network (UMIN) system (UMINStudyID: UMIN 000000559) (23). The study protocol was approved by the Ethics Committee for Human Research at Kyoto Medical Center and Tokyo Medical and Dental University. Written informed consent was obtained from all participants.

Study protocol

The study design and enrollment are shown in Supplementary Fig. 1. All of the 116 obese patients who were enrolled were also classified into those with or without dyslipidemia using the following criteria: a triglyceride (TG) level ≥1.69 mmol/L and/or HDL-cholesterol (HDL-C) <1.04 mmol/L for men and <1.29 mmol/L for women, which are some of the components of the criteria for metabolic syndrome proposed by the U.S. National Cholesterol Education Program-Adult Treatment Panel III (24), as described previously (25). Of all 90 obese patients with dyslipidemia enrolled, 8 patients dropped out (5 patients stopped consulting the outpatient clinic, and 3 patients withdrew consent). The remaining 82 patients in whom we could continue observation were assigned to the control and EPA-treated groups (Supplementary Fig. 1). This study was a prospective, randomized, open-label, blinded end point design, employing simple randomization. In the EPA-treated group, an EPA capsule (1.8 g daily) containing highly purified (>98%) EPA ethyl ester (Mochida Pharmaceutical Co., Ltd., Tokyo, Japan) was administered for 3 months, as previously described (14–17). No patients in this study had taken part in any of our previous studies. The patients' diet was based on the Japan Atherosclerosis Society Guidelines for the Diagnosis and Treatment of Atherosclerotic Cardiovascular Diseases, as previously described (14–17).

Data collection and laboratory methods

At the beginning and end of the study, we measured BMI, systolic blood pressure (SBP) and diastolic blood pressures (DBP), fasting plasma glucose (FPG), HbA_{1c}, serum immunoreactive insulin (IRI), TG, HDL-C, and LDL-cholesterol (LDL-C), adiponectin, and CRP, as previously described (14–17). The value for HbA_{1c} (%) is estimated as a National Glycohemoglobin Standardization Program equivalent value (%) calculated by the formula HbA_{1c} (National Glycohemoglobin Standardization Program) (%) = 1.02 × HbA_{1c} (Japan Diabetes Society) (%) + 0.25% (26). Serum was prepared by collecting blood into glass tubes without an anticoagulant and obtained by centrifugation (1,500 × *g*, 10 min, 4°C), and aliquots of the supernatant were frozen (−80°C) until use. The serum fatty acid levels, such as EPA and AA, were determined by capillary gas chromatography, as described elsewhere (21,22). The serum levels of IL-10 were measured using commercially available immunoassays (R&D Systems, Minneapolis, MN) (27). The mean coefficient of variance for this serum IL-10 ELISA assay shown in its manual was 5.9–7.5%. The brachial-ankle PWV was assessed using the Vasera VS-1000 vascular screening system (Fukuda Denshi, Tokyo, Japan), as described previously (10,16,23). The investigators who performed the vascular measurements were blinded to the patients' characteristics.

Peripheral blood mononuclear cells were collected from heparinized blood samples through density gradient centrifugation with lymphocyte separation solution (Nacalai Tesque, Kyoto, Japan). Human monocytes were obtained by magnetic-assisted cell sorting with anti-human CD14 immunomagnetic beads (Miltenyi Biotec, Bergisch Gladbach, Germany), and the expression of tumor necrosis factor α (TNF-α), IL-6, and IL-10 mRNA was analyzed using a real-time quantitative PCR method (9,10). Details of the primers used are described in Supplementary Materials and Methods. The percentages of $CD163^+CD14^+$ peripheral blood monocytes were analyzed by flow cytometry (FACSCanto; BD Biosciences) with human antibodies against CD14 and CD163 (BD Pharmingen) (10).

Cell culture experiments

Details of cell culture, PPARα and PPARγ silencing by small interfering RNA (siRNA), chromatin immunoprecipitation (ChIP) assays, and transient transfection and luciferase assays are described in Supplementary Materials and Methods.

Statistical analysis

The sample size was calculated with a type I error of 5%, a statistical power of 80%

Table 1—*Clinical characteristics and metabolic variables, M1/M2 markers in peripheral blood monocytes, and PWV before and after treatment with EPA*

	Control		EPA	
	Baseline	After 3 months	Baseline	After 3 months
n (male/female)	26/13		22/21	
Age (years)	54.0 ± 13		52.3 ± 13	
BMI (kg/m^2)	29.1 ± 5.3	29.0 ± 5.5	29.9 ± 4.9	29.6 ± 4.4
SBP (mmHg)	141 ± 19	137 ± 16	139 ± 18	138 ± 18
DBP (mmHg)	83.9 ± 11	83.1 ± 9	83.8 ± 11	85.6 ± 11
EPA (μg/mL)[a]	42 (27–83)	60 (28–88)	51 (31–105)	110 (87–167)**
EPA/AA[a]	0.3 (0.2–0.5)	0.4 (0.2–0.6)	0.3 (0.2–0.7)	0.8 (0.7–1.2)**
FPG (mmol/L)[a]	6.2 (5.3–7.9)	6.1 (5.3–7.6)	6.3 (5.3–7.2)	6.5 (5.4–7.4)
HbA_{1c} (%)	6.5 (5.5–7.3)	6.4 (5.6–7.0)	6.3 (6.0–7.7)	6.2 (5.8–7.4)*
IRI (pmol/L)[a]	62 (36–131)	62 (32–100)	77 (53–136)	77 (53–103)
TG (mmol/L)[a]	2.0 (1.7–2.5)	1.8 (1.4–2.5)	2.3 (1.9–3.2)	1.7 (1.5–2.3)**
HDL-C (mmol/L)	1.4 ± 0.3	1.4 ± 0.3	1.4 ± 0.3	1.4 ± 0.3
LDL-C (mmol/)	3.1 ± 0.6	3.0 ± 0.6	3.4 ± 0.8	3.2 ± 0.8
Adiponectin (μg/mL)[a]	6.5 (4.3–8.7)	6.2 (4.3–8.0)	6.1 (4.3–7.2)	6.6 (4.4–8.8)*
CRP (μg/mL)[a]	1.1 (0.5–1.9)	1.0 (0.4–1.6)	0.7 (0.5–2.5)	0.6 (0.4–1.2)
IL-10 (pg/mL)	5.1 ± 1.6	4.9 ± 1.5	5.2 ± 2.1	6.2 ±1.9**
PWV (cm/s)	1,403 ± 221	1,374 ± 206	1,476 ± 298	1,406 ± 296**
Expression in monocytes				
TNF-α (arbitrary units)[a]	1.2 (0.2–3.2)	1.4 (0.2–2.6)	2.3 (1.1–3.3)	2.3 (1.2–3.5)
IL-6 (arbitrary units)[a]	5.1 (2.6–7.6)	5.0 (3.3–7.0)	7.0 (4.6–9.6)	6.8 (4.3–9.6)
IL-10 (arbitrary units)[a]	4.7 (3.1–7.2)	5.4 (2.0–10.5)	5.5 (2.1–13.3)	10.0 (5.0–18.3)**
CD163/CD14 (%)	55.6 ± 12.5	53.4 ± 11.9	55.1 ± 13.4	57.8 ± 14.0
Proportion of				
Diabetes (%)	46.2		44.2	
Hypertension (%)	61.5		55.8	

Data are shown as the mean ± *SD* or median (interquartile range), unless otherwise noted. [a]Data were nonnormally distributed and analyzed by nonparametric Wilcoxon test. *$P < 0.05$ and **$P < 0.01$ vs. baseline measurement as determined by a two-way repeated-measures ANOVA (control and EPA groups × before and after treatment).

(type II error of 20%), and a standardized effect size of 0.67, so as to demonstrate an EPA-induced change of 1.0 pg/mL of serum IL-10 as being significant using the paired *t* test. Data are presented as the mean ± SD, unless otherwise indicated, and $P < 0.05$ was considered significant. Logarithmic transformation (ln) was used for the variables that were not normally distributed to make their distribution normal.

Student *t* test was used for comparisons of the means between the two groups at the baseline or posttreatment. Categorical variables were evaluated by the χ^2 test. A two-tailed, paired *t* test was applied to evaluate changes from the baseline to posttreatment (14,16). Some of the data were not normally distributed; therefore, in these cases, the nonparametric Wilcoxon test was used instead of the *t* test. Repeated-measures ANOVA was used to assess the effects of EPA on the measured variables. Pearson correlation coefficient was employed to investigate the correlations among M1/M2 markers, PWV, and metabolic parameters at the baseline, between these changes during the EPA treatment, and between the EPA/AA ratio and IL-10 levels after EPA treatment. Changes from the baseline to those at 3 months are abbreviated as Δ. Pearson partial correlation of ΔIL-10 expression in monocytes and ΔPWV with Δmetabolic parameters during EPA treatment was adjusted for the age, sex, and each initial value. ΔIL-10 expression in monocytes was adjusted for the age, sex, and initial IL-10 expression in monocytes, and, in the case of ΔPWV, it was adjusted for the age, sex, and initial values of SBP and PWV. For in vitro studies, post hoc analysis was performed using the Tukey-Kramer test for the comparison among all groups or Dunnett method for the comparison of specific groups. All analyses were performed using Stat View version 5.0 for Windows (SAS Institute Inc., Cary, NC) and SPSS 12.0 for Windows (SPSS Inc., Chicago, IL).

RESULTS

Baseline characteristics of obese patients with or without dyslipidemia

A summary of the characteristics of the study cohort and a comparison of the obese patients with or without dyslipidemia are shown in Supplementary Table 1. Of all of the 116 obese patients (64 men and 52 women; mean age, 50.9 years), there were 90 (77.6%) obese patients with dyslipidemia. There were no significant differences in age, BMI, SBP, DBP, FPG, HbA_{1c}, IRI, LDL-C, CRP, PWV, and proportion of diabetes and hypertension between those with and without dyslipidemia. The levels of EPA and the EPA/AA ratio tended to be, but not significantly, lower in obese patients with than in those without dyslipidemia (Supplementary Table 1). The serum levels of TG were significantly higher, and those of HDL-C, adiponectin, and IL-10 were significantly lower in obese patients with than in those without dyslipidemia (TG, HDL-C, $P < 0.01$; adiponectin, IL-10, $P < 0.05$). The obese patients with dyslipidemia exhibited significantly lower IL-10 RNA levels in the peripheral blood monocytes than those without dyslipidemia ($P < 0.05$). There were no significant differences in the expression levels of TNF-α, IL-6, and CD163 in peripheral blood monocytes between the two groups (Supplementary Table 1).

Effect of EPA treatment on metabolic syndrome–related variables, M1/M2 markers in peripheral blood monocytes, and PWV

Among 90 obese patients with dyslipidemia enrolled, 8 excluded subjects who dropped out before randomization had a relatively higher BMI and lower age, FPG, HbA_{1c}, and serum IL-10 than the remaining 82 patients. The remaining 82 obese patients with dyslipidemia in whom we could continue observation were randomly assigned to two groups: the EPA-treated group (n = 43, 22 men and 21 women; mean BMI, 29.9 ± 4.9 kg/m^2) and the untreated control group (n = 39, 26 men and 13 women; mean BMI, 29.1 ± 5.3 kg/m^2). Among the 82 obese patients with dyslipidemia, no participants dropped out of this study. With regard to the control group, all variables

Table 2—*Correlations related to changes in IL-10 in peripheral blood and PWV during treatment with EPA*

	Expression of monocytes			
	ΔIL-10		ΔPWV	
	r	r_p[a]	*r*	r_p[b]
ΔBMI	0.02	−0.01	0.08	0.10
ΔSBP	−0.03	−0.09	0.02	0.08
ΔEPA	0.25*	0.27*	0.06	0.05
ΔHbA_{1c}	−0.20	−0.17	0.05	0.05
ΔTG	−0.13	−0.13	0.19	0.15
ΔHDL-C	0.15	0.21	0.13	0.10
ΔAdiponectin	0.25*	0.22	−0.31**	−0.35**
ΔIL-10	0.01	−0.15	−0.03	0.07
Expression in monocytes				
ΔTNF-α	−0.02	−0.01	−0.07	−0.03
ΔIL-6	0.04	0.14	0.04	−0.12
ΔIL-10	—	—	−0.27*	−0.26*
ΔCD163/CD14	−0.07	−0.03	−0.08	0.07

In 82 obese patients who were assigned to the control group and EPA-treated groups, correlations related to changes in monocyte IL-10 and PWV were examined. Data are Pearson simple and partial correlation coefficients regarding changes during EPA treatment of IL-10 levels in peripheral blood monocytes and of PWV during treatment with EPA. $n = 82$ patients. [a]Value adjusted for age, sex, and initial IL-10 levels in monocytes. [b]Value adjusted for age, sex, initial systolic blood pressure, and initial PWV. *$P < 0.05$ and **$P < 0.01$.

remained unchanged throughout the study (Table 1). Treatment with EPA for 3 months caused a significant reduction of serum levels of HbA_{1c} ($P < 0.05$) and TG ($P < 0.01$) in parallel with a decrease in PWV ($P < 0.01$) and a significant increase of serum levels of EPA, the EPA/AA ratio ($P < 0.01$), and adiponectin ($P < 0.05$) in obese patients, which are consistent with our previous report (14–17). After EPA treatment, the serum level of IL-10 was also significantly increased in obese patients with dyslipidemia ($P < 0.01$). The expression levels for IL-10 RNA were significantly increased by 1.8-fold in peripheral blood monocytes from obese patients with dyslipidemia (from 5.5 to 10.0; $P < 0.05$) (Table 1). However, there were no appreciable changes in the expression levels of TNF-α, IL-6, and CD163 in peripheral blood monocytes after EPA treatment.

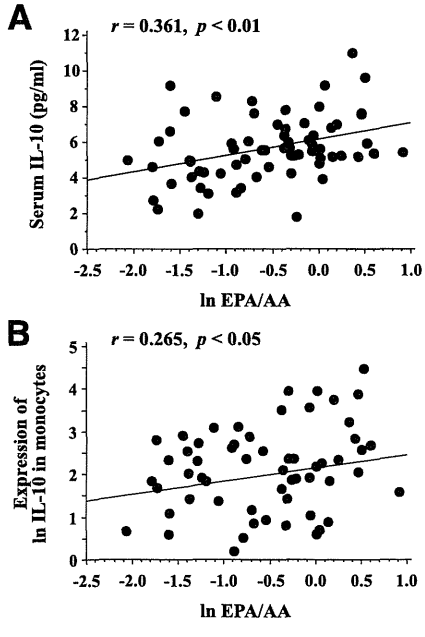

Figure 1—*Association of serum ln EPA/AA ratio with serum level of IL-10* (A) *and expression of ln IL-10 in monocytes* (B) *after 3-month treatment with EPA.*

Correlations related to changes in IL-10 in peripheral blood monocytes and PWV during treatment with EPA

Table 2 lists data for all subjects regarding the correlations observed during EPA treatment between the metabolic syndrome–related variables, IL-10 RNA levels in peripheral blood monocytes, and PWV. In all study subjects, Pearson correlation coefficient revealed that ΔTNF-α, ΔIL-6, and ΔCD163 in peripheral blood monocytes were not correlated with changes in any metabolic variable (data not shown). However, ΔIL-10 expression in peripheral blood monocytes was positively correlated with serum ΔEPA levels and serum Δadiponectin during EPA treatment ($P < 0.05$). Furthermore, ΔPWV by EPA treatment was negatively correlated only with Δadiponectin ($P < 0.01$) and ΔIL-10 expression of monocytes ($P < 0.05$) (Table 2). In addition, after adjusting for age, sex, and initial IL-10, ΔIL-10 expression in peripheral blood monocytes was positively correlated with serum ΔEPA levels during EPA treatment (partial correlation coefficient [r_p] = 0.27; $P < 0.05$). Also, ΔPWV during EPA treatment was negatively correlated only with Δadiponectin ($r_p = -0.35$; $P < 0.01$) and ΔIL-10 expression of monocytes ($r_p = -0.26$; $P < 0.05$) after adjusting for the age, sex, and initial SBP and PWV (Table 2).

Association of serum EPA/AA ratio with serum level of IL-10 and expression of IL-10 in monocytes after EPA treatment

The serum ln EPA/AA ratio after EPA treatment was significantly correlated with the serum IL-10 level and expression level of ln IL-10 in monocytes after EPA treatment (serum IL-10, $r = 0.361$, $P < 0.01$; ln IL-10 expression in monocytes, $r = 0.265$, $P < 0.05$) (Fig. 1*A* and *B*).

Effects of EPA treatment in cultured human monocytic THP-1 cells

To explore the direct effect of EPA on the RNA expression of IL-10, human monocytic THP-1 cells were incubated with 0, 10, or 50 μmol/L EPA for 24 h and stimulated with LPS for 6 h. The expression of IL-10 in THP-1 cells stimulated with LPS was twofold higher than that in THP-1 cells without LPS stimulation ($P < 0.05$) (Fig. 2*A*). Treatment with EPA for 24 h in THP-1 cells with LPS increased the expression of IL-10 in a dose-dependent manner. Treatment with 10 μmol/L EPA significantly increased the expression of IL-10 compared with that without EPA ($P < 0.05$), and treatment with 50 μmol/L EPA significantly increased the expression of IL-10 compared with that without EPA or with 10 μmol/L EPA in THP-1 cells stimulated with LPS ($P < 0.01$) (Fig. 2*A*). We also observed that treatment with 50 μmol/L EPA for 24 h significantly increased the levels of IL-10 protein in medium compared with that without EPA and 10 μmol/L EPA in THP-1 cells stimulated with LPS ($P < 0.01$) (Fig. 2*B*).

Effects of PPAR antagonists on EPA-induced increase of IL-10 expression

We examined whether the effects of EPA on IL-10 expression in THP-1 cells were dependent on PPARα or PPARγ. Incubation of cultures with PPARγ-specific antagonists T0070907 or GW9662 significantly blocked the effect of the treatment with EPA for 24 h on IL-10 expression induced by LPS ($P < 0.05$), whereas the incubation of cultures with the PPARα-specific antagonist MK-886 did not block the effect of EPA on IL-10 expression (Fig. 2*C*). The increased levels of IL-10 protein in medium due to treatment with EPA for 24 h were also blocked with PPARγ-specific antagonists T0070907 and GW9662 ($P < 0.01$), but not with the PPARα-specific antagonist MK-886 (Fig. 2*D*). These findings suggest that EPA exerts anti-inflammatory effects through a PPARγ-dependent pathway.

Effects of EPA on expression of IL-10 in PPAR knockdown THP-1 cells

We used PPARα and PPARγ silencing for further elucidation of the mechanism of action of EPA on the increased expression of IL-10 in THP-1 cells. Treatment with 50 μmol/L EPA, which is within the physiological range observed in study subjects, significantly increased the expression of IL-10 compared with that without EPA ($P < 0.01$). PPARγ knockdown resulted in a loss of EPA-mediated IL-10 production ($P < 0.01$), whereas PPARα knockdown did not alter the effect of EPA on IL-10 expression (Fig. 2*E*). The efficiency of PPARα and PPARγ silencing in THP-1 cells was determined by Western blot analysis, in which decreased expressions of PPARα and PPARγ were observed, respectively. PPARα– and PPARγ–siRNA effectively decreased PPARα and PPARγ levels by ~70% compared with scrambled (nonsilencing) siRNA ($P < 0.05$) (Fig. 2*F*).

Effect of EPA on human IL-10 promoter

In order to examine the effects of EPA on the IL-10 promoter in THP-1 cells, two THP-1 IL-10 promoter luciferase reporter gene constructs, the first containing the IL-10 promoter sequences −421/+120 (pGL3-P421) and the second containing sequences −384/+120 (pGL3-P384), were generated. After 6 h of treatment with LPS (20 ng/mL), the ability of EPA to increase luciferase transcription was assessed. Treatment with EPA (50 μmol/L) significantly ($P = 0.0013$) increased the activity of pGL3-P421 2.4-fold, but did not increase the pGL3-P384 activity (1.2-fold) (Fig. 2*G*). The IL-10 promoter contains peroxisome proliferator response element (PPRE) at −406/−390. These findings indicate that EPA activates the transcription of IL-10, and that IL-10 promoter sequences −421/−384 containing PPRE are required for this activation.

Effect of EPA on binding of PPARγ to IL-10 promoter

To evaluate the influence of EPA on the binding of PPARγ to the endogenous IL-10 promoter in THP-1 cells, ChIP assays were performed. Fig. 2*H* shows the results of quantitative analysis of PCR amplification products before and after the immunoprecipitation of the cross-linked chromatin with anti-PPARγ antibody. These results demonstrate that PPARγ is recruited to the region containing the PPRE site (−406/−390) of the endogenous IL-10 promoter (*lane 5*). In addition, EPA treatment markedly enhanced the PCR amplification product of IL-10, displaying an EPA-induced increase in the binding of PPARγ to the IL-10 promoter (*lane 6*). In contrast, before immunoprecipitation, levels of the IL-10 promoter region containing PPRE were similar between chromatins from cells stimulated with and without EPA (*lanes 1* and *2*, respectively). No PCR-amplified product was found following the immunoprecipitation of the cross-linked chromatin with normal rabbit IgG (*lanes 3* and *4*). PCR amplification with specific primers for the GAPDH gene did not result in significant signals in any immunoprecipitated samples (data not shown), demonstrating the specificity of immunoprecipitation and PCR reactions. These data support the idea that EPA significantly increased the binding of PPARγ to the IL-10 promoter sequences containing PPRE in THP-1 cells.

CONCLUSIONS—In a subanalysis of the JELIS, EPA led to a greater reduction in the risk of coronary artery disease by up to 53% in patients with high TG and low HDL-C levels, two of the risk factors of metabolic syndrome and cardiovascular disease (25). However, this mechanism is still poorly understood.

The current study revealed that levels of IL-10, an anti-inflammatory M2 marker, in monocytes were significantly lower in obese patients with than in those without dyslipidemia. Our data are compatible with a previous report by Esposito et al. (28) showing that serum IL-10 levels were lower in obese women with metabolic syndrome than in those without metabolic syndrome. As IL-10 downregulates the production of proinflammatory cytokines, it is tempting to speculate that the low IL-10 levels observed in obese patients with dyslipidemia represent an attempt to promote continued proinflammatory cytokine production. We also demonstrated for the first time that EPA significantly increases the IL-10 levels in monocytes and serum of obese dyslipidemic patients. These findings indicate that EPA ameliorated the decreased IL-10 RNA levels in monocytes of obese patients with dyslipidemia. This finding is also consistent with the report by Oh et al. (29), demonstrating that fish oil supplementation increases adipose tissue expression of M2 markers, including IL-10, in obese mice. Given the anti-inflammatory and antiatherogenic properties of IL-10 produced by Th2 cytokines (4,11), our results suggest that an EPA-induced improvement of decreased IL-10 RNA levels in monocytes of obese dyslipidemic patients might lead to greater cardioprotective effects of EPA.

In this study, we also confirmed that 3-month treatment with EPA effectively improved PWV, an index of arterial stiffness, as we previously reported (16). Pearson partial correlation in this study revealed that only increased monocyte IL-10 RNA and serum adiponectin levels were significantly correlated with the reduction of PWV by EPA treatment. Recently, it was indicated that cell heterogeneity (M1/M2-like phenotype, especially an increased M1/M2 ratio) of circulating monocytes may influence their ability to attach to endothelial cells and increase plaque formation of atherosclerotic lesions (7,8). IL-10 has also been reported to promote the differentiation of M2 macrophages and attenuate the M1 macrophage population (30). Further, it was reported that the increased IL-10 signaling elicits the differentiation or recruitment of alternative M2 macrophages in adipose tissue in mice, thus contributing to reducing inflammation and improving insulin signaling (11). Previous studies demonstrated that IL-10–transgenic mice or gene transfer of IL-10 reduced atherosclerosis in C57BL/6J mice or murine atherosclerotic models (31,32), whereas their IL-10–deficient counterparts exhibited increased early

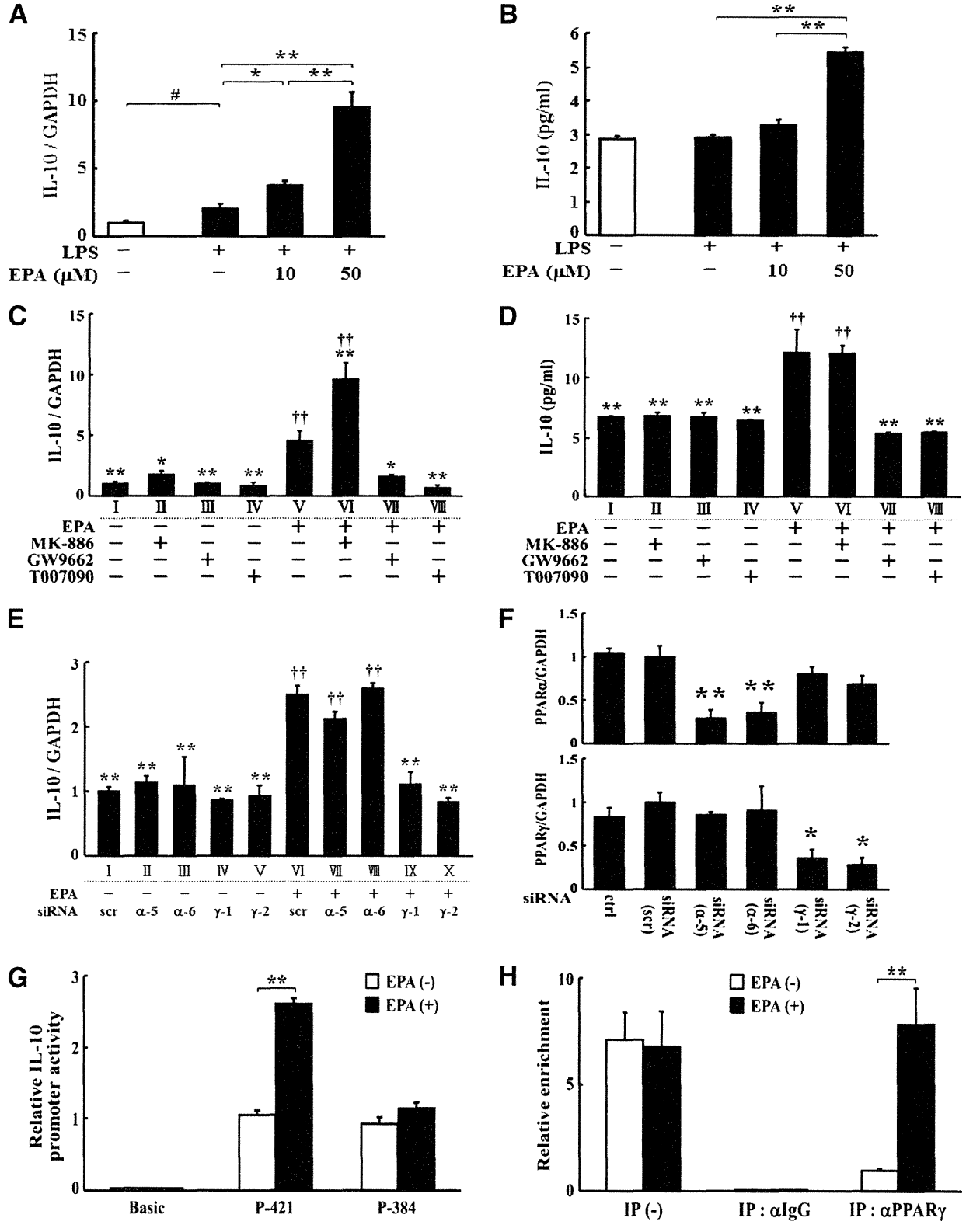

Figure 2—*Effects of EPA treatment in cultured human THP-1 cells.* A *and* B: *Effects of EPA treatment on IL-10 mRNA and protein levels in medium of cultured THP-1 cells. Data are the mean ± SE. Differences between the groups treated with and without LPS within EPA-untreated cells were assessed by Student* t *test. Differences between groups within LPS-treated THP-1 cells were assessed using the Tukey-Kramer post hoc test* (n = 6–8). *IL-10 mRNA expression* (A) *and IL-10 protein levels in medium* (B) *in THP-1 monocytes after treatment without or with 10 or 50 μmol/L EPA for*

atherosclerotic lesion formation (31). In addition, IL-10 overexpression in macrophages inhibited atherosclerosis in LDL receptor-deficient mice (33). Taken together, these findings provide evidence that IL-10 is an important key factor for the prevention of atherosclerosis in vivo. The effect of EPA on IL-10 of monocytes might be attributable to the beneficial effect on arterial stiffness of EPA. However, further examination is necessary to elucidate the causal relationship between an increase of IL-10 expression and the improvement in vascular function by EPA.

Even excluding the influence of age, sex, and the initial value of IL-10 expression in monocytes, only the ΔEPA level was significantly positively correlated with ΔIL-10 expression in monocytes during EPA treatment. In human monocytic THP-1 cells, we found that EPA increased the mRNA expression and protein levels of IL-10 in the medium. In this study, in vitro analysis using PPAR antagonists and siRNA revealed that EPA increased the expression of IL-10 through PPARγ, but not PPARα, in THP-1 cells. This finding is consistent with a previous report showing that EPA decreased IL-6 production through PPARγ, not through PPARα, in C6 glioma cells (34). We have also performed ChIP and luciferase assays to elucidate how EPA regulates IL-10 expression through a PPARγ-dependent pathway. Luciferase assays showed that EPA activates the transcription of IL-10 and that IL-10 promoter sequences containing PPRE are required. In addition, ChIP assays revealed that EPA significantly increased the binding of PPARγ to the IL-10 promoter sequences containing PPRE in THP-1 cells. These results are similar to the findings of a previous study using rosiglitazone, one of the PPARγ ligands (35). From these findings, it is conceivable that EPA increases the binding of PPARγ to the human IL-10 promoter region and activates transcription of the human IL-10 gene. As reported previously, EPA, via the activation of PPARγ, mediates various actions such as the inhibition of IL-6 production in C6 glioma cells and of MMP expression in macrophages and the increase of adiponectin expression in adipocytes (34,36,37). Moreover, PPARγ expression itself has been reported to be significantly associated with increased M2 monocytes in the vasculature and maturation of alternatively activated macrophages (6,8). We also observed that pioglitazone, a PPARγ agonist, increased IL-10 expression and improved the unbalanced M1/M2-like phenotype of monocytes in obese diabetic patients, which may contribute to its antiatherogenic effect (10). Therefore, our findings indicate that the upregulation of IL-10 induced by EPA is potentially mediated in part through the activation of PPARγ. However, further studies on the direct interaction between EPA and PPARγ, such as identification of the binding site using X-ray analysis, are required to clarify whether EPA is a functional ligand of PPARγ.

We revealed that the EPA-induced increase of adiponectin was also significantly negatively correlated with the improvement of PWV through EPA treatment. We previously demonstrated that EPA increases adiponectin in obese mice and obese human subjects, possibly through improvement of the inflammatory changes in obese adipose tissue (15). Previous epidemiological studies reported a significant positive correlation between serum adiponectin and IL-10 in healthy and obese subjects (27). In human monocyte-derived macrophages, adiponectin significantly increased the expression and secretion of IL-10 (38). Recently, Ohashi et al. (39) reported that adiponectin promotes macrophage polarization toward an anti-inflammatory phenotype, which may be partly linked to the decrease of arterial stiffness in our study. Collectively, it is conceivable that EPA increases IL-10 RNA expression of monocytes in hyperinsulinemic obese patients, in part through the enhancement of adiponectin by EPA, thereby additively suppressing the atherogenic process.

The current study showed that EPA treatment significantly increased the serum EPA/AA ratio. In addition, the EPA/AA ratio after EPA treatment was significantly correlated with IL-10 in monocytes. Recently, it was reported that a lower level of EPA was an independent predictor of all-cause-mortality in patients with acute myocardial infarction (40). EPA can be metabolized to anti-inflammatory eicosanoids and also partially replace the AA in cell membranes and competitively inhibits the production of AA and inflammatory eicosanoids, thereby exerting an anti-inflammatory effect (20). There is also a recent report showing that the serum EPA levels and

*24 h and subsequent stimulation with LPS for 6 h. The mRNA levels of IL-10 (A) were measured using quantitative real-time PCR and standardized for the GAPDH levels. #P < 0.05 by Student t test; *P < 0.05, **P < 0.01 using the Tukey-Kramer method. C and D: Effect of PPARα and PPARγ antagonists on IL-10 mRNA expression and IL-10 protein levels in cultured THP-1 cells. THP-1 monocytes with a density of 1 × 10^6 cells/well were treated with LPS for 6 h in the absence or presence of 50 μmol/L EPA for 24 h. Some cultures were incubated with the PPARα antagonist MK-886 (II, VI), and some with the PPARγ agonists GW9662 (III, VII) or T0070907 (IV, VIII), at a dose of 10 μmol/L in the presence of LPS. The expressions of IL-10 mRNA in THP-1 cells (C) and IL-10 protein levels in medium (D) were compared with those of cultures incubated without PPAR antagonists in the absence (I) or presence (V) of 50 μmol/L EPA. ††P < 0.01 vs. group I; *P < 0.05, **P < 0.01 vs. group V using the Dunnett method (n = 4–6). E and F: Effects of EPA on IL-10 expression by PPAR knockdown in THP-1 cells. Incubation was conducted with scrambled siRNA (scr), PPARα–siRNA (α-5, α-6), or PPARγ–siRNA (γ-1, γ-2) during THP-1 differentiation into macrophages, as described in RESEARCH DESIGN AND METHODS. After treatment with siRNA (25 nmol/L), EPA (50 μmol/L), and LPS, cells were harvested, and the mRNA levels of IL-10 were measured by real-time PCR (E). The protein levels of PPARα and PPARγ were measured using Western blot analysis, and quantitative data are expressed as the fold of the control scrambled siRNA and are the mean ± SE (F). Expression levels were standardized for GAPDH levels. The results of three separately performed experiments are expressed relative to the control and presented as the mean ± SE. ††P < 0.01, vs. group I; **P < 0.01 vs. group VI by the Dunnett method (E). *P < 0.05, **P < 0.01 vs. scr by the Dunnett method (F). G and H: Effects of EPA on human IL-10 promoter and on binding of PPARγ to IL-10 promoter. G: Luciferase reporter assays were performed using the luciferase reporter constructs for the human IL-10 promoter. Cells were transiently transfected with either pGL3-P421 (P-421) or pGL3-P384 (P-384) and the control plasmid pRL-TK. After 24 h, cells were treated with EPA (50 μmol/L) for 24 h and were stimulated by LPS (20 ng/mL) for 6 h. Luciferase activity was measured using a luminometer, and the results were normalized against the* Renilla *luciferase control. **P < 0.01 vs. cells treated without EPA using Student t test. H: IL-10 promoter ChIP assays were performed using chromatin extracts prepared from THP-1 monocytes treated with or without EPA (50 μmol/L) for 24 h and were stimulated by LPS (20 ng/mL) for 6 h. Control PCRs were carried out with nonimmunoprecipitated genomic DNA [input: IP(-)]. ctrl, control; αIgG indicates anti-rabbit IgG; αPPARγ, anti-PPARγ antibody. **P < 0.01 vs. cells treated without EPA using Student t test.*

AA/EPA ratio were significantly associated with the extent of coronary soft plaques and calcification (21). Furthermore, subanalysis of the JELIS has shown that the EPA/AA ratio is markedly correlated with a lower incidence of sudden cardiac death and myocardial infarction (22). Because EPA competitively inhibits inflammatory eicosanoids produced by AA (20), these findings raise the possibility that the EPA-induced increase of IL-10 RNA levels in monocytes is at least partially caused by inhibition of the proinflammatory effects of AA by EPA.

There are some limitations regarding the current study. Because Pearson correlation coefficients in this study are relatively weak, it is necessary to conduct a long-term prospective cohort study with a larger sample size in order to clarify the involvement of monocyte IL-10 in the improvement of vascular function by the treatment with EPA. Several lines of evidence suggest the important role of monocyte heterogeneity for the local macrophage conditions and inflammation in atherosclerotic lesions in mouse (7,8). However, further investigation is needed to elucidate whether the M1/M2-like phenotype or a higher IL-10 level of circulating monocytes reflects the M1/M2 macrophages and contributes to disease progression in atherosclerotic lesions in human.

In conclusion, this study demonstrates that EPA increases the IL-10 expression in peripheral blood monocytes in parallel with the decrease of arterial stiffness in obese patients with dyslipidemia. Given the anti-inflammatory and antiatherogenic properties of IL-10 (4,11), the beneficial antiatherogenic effect of EPA may be due, at least in part, to increased IL-10 expression and secretion in monocytes. As EPA is a specific n-3 PUFA that has been proven to reduce the risk of major coronary events (13), the results of this study provide important insights into its therapeutic implications in obesity-related atherosclerotic diseases.

Acknowledgments—This work was supported in part by a Grant-in-Aid for Scientific Research from the Ministry of Education, Culture, Sports, Science, and Technology of Japan; the Ministry of Health, Labour, and Welfare of Japan; and grants from the National Hospital Organization for collaborative clinical research, Kao Research Council for the Study of Healthcare Science, and the Smoking Research Foundation (to N.S.-A.).

No potential conflicts of interest relevant to this article were reported.

N.S.-A. researched the data, contributed to the discussion, wrote the manuscript, and reviewed and edited the manuscript. A.S. contributed to the discussion and reviewed and edited the manuscript. Y.S. researched the data, contributed to the discussion, and reviewed and edited the manuscript. H.N., A.H., and M.T. researched the data. S.K. and H.W. contributed to the discussion. T.T. researched the data. K.O. researched the data and contributed to the discussion. T.S. and Y.O. contributed to the discussion and reviewed and edited the manuscript. K.H. contributed to the discussion, wrote the manuscript, and reviewed and edited the manuscript. N.S.-A. is the guarantor of this work and, as such, had full access to all the data in the study and takes responsibility for the integrity of the data and the accuracy of the data analysis.

The authors thank Hajime Yamakage, Keiko Muraki, and Kazuya Muranaka (all from Kyoto Medical Center) for technical assistance.

References

1. Weisberg SP, McCann D, Desai M, Rosenbaum M, Leibel RL, Ferrante AW Jr. Obesity is associated with macrophage accumulation in adipose tissue. J Clin Invest 2003;112:1796–1808
2. Suganami T, Nishida J, Ogawa Y. A paracrine loop between adipocytes and macrophages aggravates inflammatory changes: role of free fatty acids and tumor necrosis factor alpha. Arterioscler Thromb Vasc Biol 2005;25:2062–2068
3. Gordon S, Taylor PR. Monocyte and macrophage heterogeneity. Nat Rev Immunol 2005;5:953–964
4. Lumeng CN, Bodzin JL, Saltiel AR. Obesity induces a phenotypic switch in adipose tissue macrophage polarization. J Clin Invest 2007;117:175–184
5. Lumeng CN, DelProposto JB, Westcott DJ, Saltiel AR. Phenotypic switching of adipose tissue macrophages with obesity is generated by spatiotemporal differences in macrophage subtypes. Diabetes 2008; 57:3239–3246
6. Odegaard JI, Ricardo-Gonzalez RR, Goforth MH, et al. Macrophage-specific PPARgamma controls alternative activation and improves insulin resistance. Nature 2007;447:1116–1120
7. Swirski FK, Weissleder R, Pittet MJ. Heterogeneous in vivo behavior of monocyte subsets in atherosclerosis. Arterioscler Thromb Vasc Biol 2009;29:1424–432
8. Bouhlel MA, Derudas B, Rigamonti E, et al. PPARgamma activation primes human monocytes into alternative M2 macrophages with anti-inflammatory properties. Cell Metab 2007;6:137–143
9. Ghanim H, Aljada A, Hofmeyer D, Syed T, Mohanty P, Dandona P. Circulating mononuclear cells in the obese are in a proinflammatory state. Circulation 2004; 110:1564–1571
10. Satoh N, Shimatsu A, Himeno A, et al. Unbalanced M1/M2 phenotype of peripheral blood monocytes in obese diabetic patients: effect of pioglitazone. Diabetes Care 2010;33:e7
11. Fujisaka S, Usui I, Bukhari A, et al. Regulatory mechanisms for adipose tissue M1 and M2 macrophages in diet-induced obese mice. Diabetes 2009;58:2574–2582
12. Kris-Etherton PM, Harris WS, Appel LJ; American Heart Association. Nutrition Committee. Fish consumption, fish oil, omega-3 fatty acids, and cardiovascular disease. Circulation 2002;106:2747–2757
13. Yokoyama M, Origasa H, Matsuzaki M, et al.; Japan EPA lipid intervention study (JELIS) Investigators. Effects of eicosapentaenoic acid on major coronary events in hypercholesterolaemic patients (JELIS): a randomised open-label, blinded endpoint analysis. Lancet 2007;369:1090–1098
14. Satoh N, Shimatsu A, Kotani K, et al. Purified eicosapentaenoic acid reduces small dense LDL, remnant lipoprotein particles, and C-reactive protein in metabolic syndrome. Diabetes Care 2007;30: 144–146
15. Itoh M, Suganami T, Satoh N, et al. Increased adiponectin secretion by highly purified eicosapentaenoic acid in rodent models of obesity and human obese subjects. Arterioscler Thromb Vasc Biol 2007; 27:1918–1925
16. Satoh N, Shimatsu A, Kotani K, et al. Highly purified eicosapentaenoic acid reduces cardio-ankle vascular index in association with decreased serum amyloid A-LDL in metabolic syndrome. Hypertens Res 2009;32:1004–1008
17. Yamada H, Yoshida M, Nakano Y, et al. In vivo and in vitro inhibition of monocyte adhesion to endothelial cells and endothelial adhesion molecules by eicosapentaenoic acid. Arterioscler Thromb Vasc Biol 2008;28:2173–2179
18. Renier G, Skamene E, DeSanctis J, Radzioch D. Dietary n-3 polyunsaturated fatty acids prevent the development of atherosclerotic lesions in mice. Modulation of macrophage secretory activities. Arterioscler Thromb 1993;13:1515–1524
19. Michaud SE, Renier G. Direct regulatory effect of fatty acids on macrophage lipoprotein lipase: potential role of PPARs. Diabetes 2001;50:660–666
20. Calder PC. Polyunsaturated fatty acids and inflammatory processes: New twists in an old tale. Biochimie 2009;91:791–795
21. Ueeda M, Doumei T, Takaya Y, et al. Serum N-3 polyunsaturated fatty acid levels correlate with the extent of coronary plaques and calcifications in patients with acute myocardial infarction. Circ J 2008; 72:1836–1843
22. Matsuzaki M, Yokoyama M, Saito Y, et al.; JELIS Investigators. Incremental effects of